



ELSEVIER

Forest Ecology and Management 128 (2000) 121–127

Forest Ecology  
and  
Management

www.elsevier.com/locate/foreco

## Multifractal analysis of canopy height measures in a longleaf pine savanna

Jason B. Drake<sup>a,b</sup>, John F. Weishampel<sup>a,\*</sup>

<sup>a</sup>Department of Biology, University of Central Florida, Orlando, FL 32816-2368, USA

<sup>b</sup>Department of Geography, University of Maryland, College Park, MD 20742, USA

Accepted 24 September 1999

### Abstract

Spatial patterns of forest canopies are fractal as they exhibit variation over a continuum of scales. A measure of fractal dimension of a forested landscape represents the spatial summation of physiologic (leaf-level), demographic (population-level), and abiotic (e.g., edaphic) processes, as well as exogenous disturbances (e.g., fire and hurricane) and thus provides a basis to classify or monitor such systems. However, forests typically exhibit a spectrum of fractal parameters which yields further insight to the geometric structure of the system and potentially the underlying processes. We calculated multifractal properties of longleaf pine flatwoods, the predominant ecosystem of central Florida, from canopy profile data derived from an airborne laser altimeter and ground-based measurements in The Nature Conservancy's Disney Wilderness Preserve located near Kissimmee, Florida. These metrics were compared for six  $\approx 500$  m transects to determine the level of consistency between remotely sensed and field measures and within a forest community. Multifractal techniques uncovered subtle differences between transects that could correspond to unique, underlying abiotic and biotic processes. These techniques should be considered a valuable tool for ecological analysis. © 2000 Elsevier Science B.V. All rights reserved.

*Keywords:* Canopy height; Fractals; Laser altimetry; Longleaf pine; Multifractals; Spatial pattern

### 1. Introduction

Many ecological processes (e.g., species growth, invasion, competition, facilitation, mortality) are dictated by existing spatial conditions (i.e., both biotic and abiotic) and lead to the generation of new spatial conditions (see Tilman and Kareiva, 1997). Hence, pattern and process are perpetually intertwined. In

order to understand how nature works, ecologists must be able to classify patterns and develop process-based, spatially explicit models that can produce observed patterns at multiple scales.

Recognizing the limitations of Euclidean geometry to describe natural features (e.g., tree crowns, forest patches, or landscapes), fractal geometry has been embraced by forest (e.g., Zeide, 1991; Lorimer et al., 1994; Vedyushkin, 1994) and landscape (e.g., Milne, 1991) ecologists to quantify spatial patterns. However, just as classical geometry is unable to accurately depict many natural structures (e.g., the

\* Corresponding author. Tel.: +1-407-823-6634; fax: +1-407-823-5769.

E-mail address: jweisham@mail.ucf.edu (J.F. Weishampel).

shape of a fern or the coastline of Florida), traditional fractal analysis techniques may also fall short in fully describing natural patterns. Upon closer examination of a pattern it is possible to find subsets that may have their own unique, local scaling exponents. Thus, it is often found that there are fractals embedded within fractals. These patterns, termed multifractals (Mandelbrot, 1988), are associated with nonlinear phenomena such as fluid turbulence, galaxy clustering, and the dynamics of forested systems (Solé and Manrubia, 1995) and are being detected and analyzed in remotely sensed and geospatial data (Pachepsky et al., 1997; Pecknold et al., 1997).

Our objectives were to characterize patterns of canopy height measures in a longleaf pine savanna in Central Florida. We compared these patterns of canopy height measured from both a laser altimeter and with ground-based techniques to determine the level of consistency between remotely sensed and field measures and within a forest community. Multifractal analysis can be used to characterize patterns resulting from ecological processes which operate across a wide spectrum of time-scales.

## 2. Methods

### 2.1. Remotely sensed and field measurements

Transects of laser pulse returns from the Scanning Lidar Imager of Canopies by Echo Recovery (SLI-

CER; Blair and Harding, 1998) were acquired from the Disney Wilderness Preserve (DWP) after leaf off in November 1995 (Weishampel et al., 1997). The DWP is a  $\approx 4600$  ha preserve located in central Florida straddling the Osceola/Polk county line (Fig. 1). It was conceived as a mitigation site for wetland disturbance by the Walt Disney World Corporation and the Greater Orlando Aviation Authority in early 1990s. Since then, the former cattle ranch has undergone extensive hydrological/vegetation restoration. It is comprised of patches of wetlands (e.g., bayhead swamps and cypress domes) in a matrix of more xeric upland, savanna-esque communities (e.g., pine and scrubby flatwoods).

The SLICER flight line consists of five across-track circular laser footprints 10–12 m in diameter nominally spaced 10 m along and across the flight track. The footprint diameter which is roughly equivalent to the crown width of a mature longleaf pine was a function of the beam divergence and the altitude of the plane; footprint spacing was defined by the aircraft ground speed and the laser pulse repetition rate. The larger footprint size compared to earlier altimeters (e.g., Nelson et al., 1988) increases the likelihood of recording the crown apex. Three parallel along-track transects, separated by a 10 m footprint, were divided into six, contiguous 50 footprint segments which intercepted the upland vegetation classified as pine or scrubby flatwoods. These open, fire-driven communities which dominate the preserve and much of

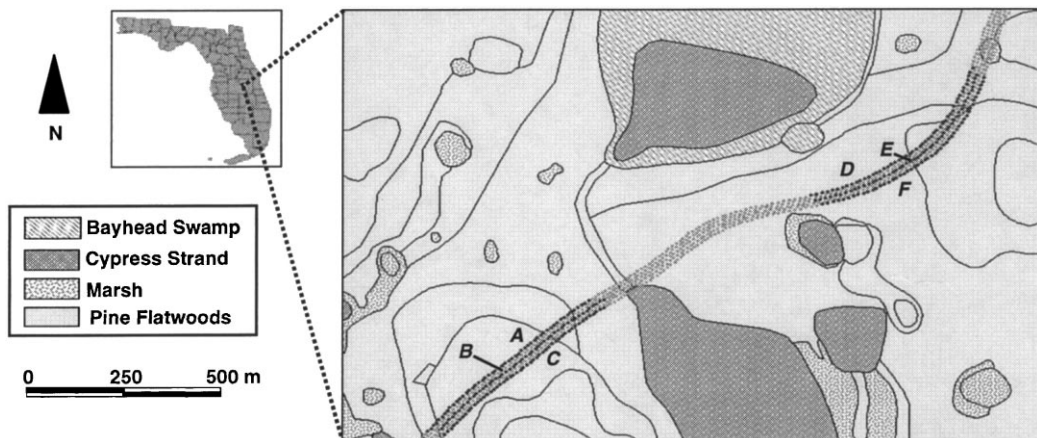


Fig. 1. SLICER flightline through Disney Wilderness Preserve (DWP) consisting of five transects of laser pulses. Sections of the studied transects are highlighted and labeled A–F.

central Florida are characterized by a longleaf pine (*Pinus palustris* Mill.) overstory and an understory comprised largely of saw palmetto (*Serenoa repens* Bartr.) and wiregrass (*Aristida stricta* Michx.) with scattered gallberry (*Ilex glabra* L.) and oak (e.g., *Quercus myrtifolia* Willd., *Q. chapmanii* Sarg.) shrubs.

The laser altimeter developed at NASA Goddard Space Flight Center was flown aboard the NASA Wallops Flight Facility T-39 Sabreliner aircraft. The onboard kinematic GPS, the inertial navigation system, and the laser respectively provided information on the aircraft position, laser pointing direction, and distance to the ground which permitted the ground location of each pulse to a horizontal accuracy of approximately 10 m. The center of each footprint in the six segments was located using a real-time differential correcting Trimble Pro-XR GPS. At these locations, the highest leaf/branch in each 10 m diameter cylinder projected above the footprint was determined using a clinometer and a sonic range finder. The SLICER waveform has a vertical resolution of 11 cm; canopy height estimates were derived with software developed by Lefsky (1997) for ground detection.

## 2.2. Multifractal analysis

### 2.2.1. Derivation of multifractal methodology

Standard fractal analysis techniques generally involve examining the change in a measure over a range of scales. Thus at finer scales, more and more mass (or density) is quantified. One technique often utilized is box counting, where the number of occupied boxes are counted at a range of different box sizes. A typical formula for fractal analysis using this method is:

$$D_f = - \lim_{\epsilon \rightarrow 0} \frac{\log N(\epsilon)}{\log \epsilon} \quad (1)$$

where  $N$  is the number of occupied boxes of size  $\epsilon$  and  $D_f$  the fractal dimension.

However, not all boxes in the grids contain equal measures so averaging these subsets eliminates potentially valuable information that could shed light on the underlying pattern-generating processes. Finer examination of patterns may reveal that each subset has different scaling exponents. These patterns are often

termed multifractals and are a composition of many fractal sets. Multifractal sets involve a spectrum of scaling indices; the mass or density around different points is characterized by different (local) fractal ‘dimensions’ or measures. Thus, multifractals may be thought of as fractals within fractals.

One way to base multifractal analysis proposed by Falconer (1990) is through the expression:

$$\Phi(q, \tau) = E \left( \sum_{i=1}^N p_i^q \epsilon_i^{-\tau} \right) \quad (2)$$

where  $q$  and  $\tau$  are real numbers and  $p_i$  and  $\epsilon_i$  are random quantities representing, respectively the measure and size factors. The sum is extended over all the separated parts,  $N$ , composing the object and  $E$  represents the expectation (or average). Thus,  $\Phi(q, \tau)$  represents the coupled moments of measure ( $q$ ) and size ( $\tau$ ).

So the transition from fractal to multifractal involves replacing the regular dimension (or scaling exponent) from Eq. (1) with a family of exponents  $\tau(q)$  (Keitt, 1996). This spectrum of scaling exponents,  $\tau(q)$ , is found by examining the power-law relationship between scale (box size,  $\epsilon$ ) and the various statistical moments ( $q$ ) of local measures on the multifractal pattern using:

$$\tau(q) = \lim_{\epsilon \rightarrow 0} \frac{\log E \sum_{i=1}^{N(\epsilon)} p_i^q(\epsilon)}{\log \epsilon} \quad (3)$$

which is often replaced by the more familiar  $\alpha(q)$  spectrum:

$$\alpha(q) = \frac{d\tau(q)}{dq} \quad (4)$$

where  $\alpha$  is called the Hölder exponent. Thus, when the family of scaling exponents,  $\alpha(q)$ , is considered over a range of  $q$  statistical moments, it is possible to illustrate how local scaling exponents differ for a given multifractal pattern. For an exact or simple fractal,  $\alpha_q = D_f$  for all  $q$ , yielding a straight-line  $\alpha(q)$  versus  $q$  graph.

Another component of multifractal analysis that is often considered is that of the  $f(\alpha)$  spectrum of multifractal measures. This spectrum can be obtained by a Legendre transform of  $\alpha$  by:

$$f(\alpha) = q\alpha - \tau \quad (5)$$

When coupled together, we may examine how the multifractal measures  $f(\alpha)$  correspond to a set of scaling exponents  $\alpha$ . In plotting  $f(\alpha)$  versus  $\alpha$ , we obtain a complete multifractal spectrum. For purely multiplicative processes this spectrum will have a concave down, parabolic shape and will have minimum and maximum  $\alpha$  values on the  $x$ -axis. The maximum  $f(\alpha)$  corresponds to the fractal dimension,  $D_f$ .

For an exact or simple fractal, not only will the  $\alpha(q)$  spectrum be the same for all  $q$  values, but the  $f(\alpha)$  versus  $\alpha$  multifractal spectrum collapses into a single point (i.e.,  $D_f$ ) (Solé and Manrubia, 1995). For a multifractal, however, the measure is different in every subset, therefore each of these has a unique scaling exponent  $\alpha$ , and associated multifractal measure  $f(\alpha)$ .

In summary, the primary focus of multifractal analysis is to consider how the measure of mass ( $p_i$ ) varies with box size ( $\varepsilon_i$ ). Another key point is to realize the importance of the range of statistical moments ( $q$ ) of local measures in discerning differences between different subsets of the overall pattern. By considering the complete spectrum of multifractal measures  $f(\alpha)$  corresponding to a set of scaling exponents  $\alpha$ , we may be able to gain insight into the local patterns embedded within a larger pattern that may be produced by ecological processes operating at very different time scales (e.g., growth, reproduction, mortality, etc). Thus, this method can substantially aid in the characterization of forest stands or landscapes.

### 2.2.2. Application of multifractals to canopy height data

Field- and lidar-detected height data from the six transects were analyzed using the multifractal techniques mentioned above using software developed by Mach and Mas (1997). For this analysis, we were interested in how the Hölder or scaling exponent ( $\alpha$ ) varied over a range (i.e., from 0.05 to 2.0 at 0.05 intervals) of the statistical moments ( $q$ ).

To test for possible nonrandom behavior in these canopy height patterns, a Monte Carlo analysis was performed. Heights from each of the transects (field- and lidar-detected) were randomly arranged along the transect 20 times and the same multifractal techniques were performed on these permuted data sets. The maximum and minimum random values were plotted against the  $\alpha(q)$  values for the field and lidar-detected transects so that significantly nonrandom ( $P < 0.05$ ) areas could be identified. To further compare the multifractal spectra of measures for both field and lidar-detected height transects from the longleaf pine community, we plotted the multifractal measures  $f(\alpha)$  against their associated scaling exponents,  $\alpha$ .

## 3. Results

The  $\alpha(q)$  spectra of scaling indices plotted over a range of  $q$  values for each of the six field- and lidar-detected canopy height transects are shown in Fig. 2. The letters (A–F) found at the beginning of each

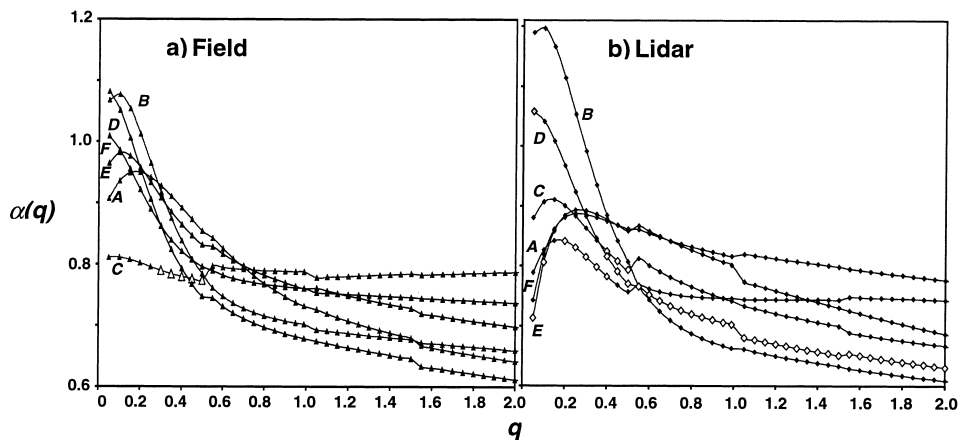


Fig. 2. (a) Field ( $\blacktriangle$ )- and (b) lidar ( $\blacklozenge$ )-detected canopy height  $\alpha(q)$  vs.  $q$  spectra of scaling indices. Open markers represent  $\alpha(q)$  values that fell outside the 95% random envelopes.

spectrum correspond to the transect letters shown in Fig. 1. Overall, the values of  $\alpha(q)$  exhibited the most change with  $q$  values below 1.0. In general, the range in  $\alpha(q)$  for low  $q$  values for the six transects was greater for the lidar estimates of canopy height. Values of  $\alpha(q)$  for a specific  $q$  that fell outside the Monte Carlo envelopes are designated with empty markers. Only field-measured canopy height transect D had  $\alpha(q)$  values below the 95% confidence envelope (Fig. 2a). Lidar-detected canopy height transects A, B, D, and F all had measures that were out of the range of spectra for randomized patterns (Fig. 2b). Only one  $\alpha(q)$  value, the first for transect F was found above the maximum range for the randomly permuted transects. This transect was also the only one to exhibit significantly low  $\alpha(q)$  values for high values of  $q$ .

The plots in Fig. 2 represent only part of the overall multifractal spectrum. As mentioned earlier, the  $\alpha(q)$  versus  $q$  spectrum specifically focuses on how the divergence or scaling exponent  $\alpha$  varies over differing order  $q$  values. Plotting the Legendre-transformed  $f(\alpha)$  function (Eq. (5), Fig. 3), with  $\alpha$  represents how the

multifractal measures,  $f(\alpha)$ , vary over a range of diverging exponents,  $\alpha$ . Thus, we are able to illustrate a true multifractal spectrum.

The multifractal spectra for transects A–F are shown in Fig. 3. The multifractal spectra,  $f(\alpha)$  versus  $\alpha$ , for both field-( $\Delta$ ) and lidar-( $\blacklozenge$ ) measured canopy height transects are plotted together. The maxima of these concave spectra, represented by the dashed or dotted asymptote lines, correspond to the traditional fractal dimension  $D_f$ . The  $D_f$  values for lidar and field transects differed by  $<0.02$  for all transects but B which differed by  $>0.03$ . While most measures exhibited a range of  $f(\alpha)$  values, the pattern found with field measured height for transect D resembled a simple fractal.

#### 4. Discussion and conclusion

The spectra of scaling indices (Fig. 2) illustrate similarities in both field- and lidar-detected canopy height transects. The general distributions of all spec-

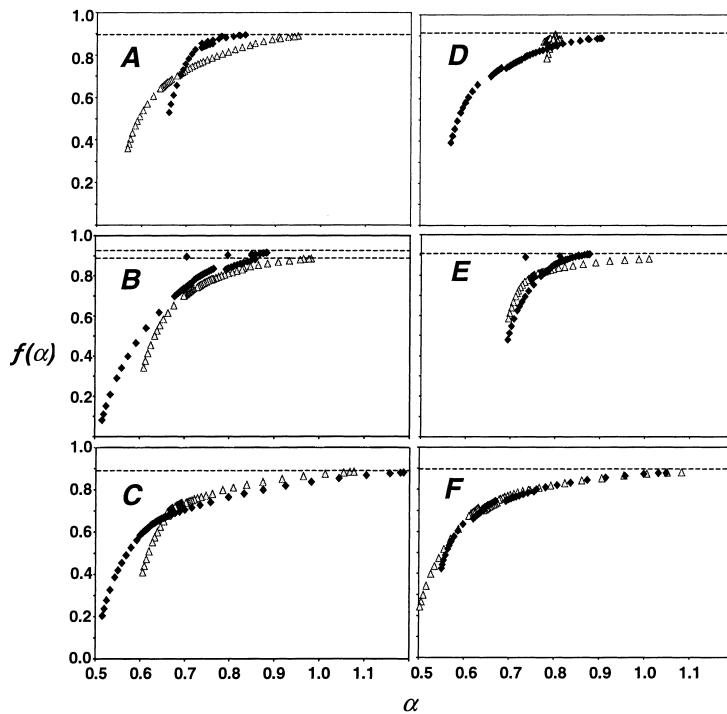


Fig. 3. Multifractal spectra for field-( $\Delta$ ) and lidar-( $\blacklozenge$ ) based height estimates. The dashed lines signify the fractal dimension, i.e., the apex of the multifractal spectra, for the different transects and canopy measurement techniques.

tra fall within a similar range of scaling exponent ( $\alpha$ ) values (0.5–1.2), which is to be expected as they are found in the same community type and therefore subject to similar abiotic and biotic factors. Variability among the  $\alpha(q)$  values was higher with smaller  $q$  values and most transects showed a peak in  $\alpha(q)$  values with  $q$ 's between 0 and 0.4. Transects C and F exhibited the highest maximum  $\alpha(q)$  values in both measurements of canopy heights. However, in general the spectra for a given field measured transect were not concordant with the spectra for the corresponding remotely sensed transect. This suggests that the laser footprint and field plot locations did not precisely coincide or the measure of highest leaf/branch does not correspond to the initial return of the laser pulse above background noise. This problem is amplified by the open nature of the longleaf pine flatwoods where a few meters discrepancy determines whether a longleaf pine ( $\approx 15$  m) or saw palmetto ( $< 1$  m) crown was hit.

Though not the classic example of light-controlled forest gap dynamics, longleaf pine savannas do exhibit a cyclical gap-phase pattern across the landscape (Brockway and Outcalt, 1998). Dispersion patterns of longleaf pine seedlings and juveniles are highly aggregated occurring in distinct, separated patches, while adults tend to be more randomly scattered (Platt et al., 1988). Thus, through mortality due to competition (for water and nutrients) and fire, the spatial patterns of cohorts change as trees mature. This tendency towards a random pattern of canopy heights may relate to Fig. 2, where the majority of  $\alpha(q)$  values fell within random envelopes.

Perhaps more interesting than the similarities are the subtle differences of these transects. For transects measured with the same technique (i.e., lidar), there are remarkable difference in local responses. For example transects B and C are found within close proximity to one another, but have very different spectra for both field and lidar measures. These differences in local scaling exponents between adjacent transects may represent the importance of local abiotic heterogeneity on patterns of canopy heights. Also an important point is to note the nearly straight line spectra found for field transect D. Since there is very little difference in local scaling exponents over a range of statistical moments, this transect appears to have self-similarity over many scales and therefore approximates a simple (mono-) fractal.

By limiting our analyses to a single fractal dimension, we would have concluded that all of these transects were essentially the same (i.e.,  $D_f = 0.89$ ). Although valid, by considering the multifractal spectra composed of various multifractal measures  $f(\alpha)$  and their associated scaling exponents ( $\alpha$ ), we uncovered local differences embedded within the transects (Fig. 3). There is an overall general agreement in the multifractal spectra of both field- and lidar-measured transects. The partial concave down shape of these multifractal spectra is indicative of nonlinear, multiplicative underlying processes (Mandelbrot, 1988). These processes in general are responsible for the transition from a pattern characterized by a single fractal dimension into one characterized by a multifractal spectrum. An exception to this is found for field transect D, which appears to have little more than a single point representing its spectrum, resembling a monofractal. By examining the asymptotes it is clear that (a) nearly all transects have the same regular fractal dimension ( $D_f$ ) and (b) this technique is uncovering a great deal of information regarding the fine scale differences in pattern within these transects. These differences in pattern could relate to subtle differences in abiotic and biotic processes.

Multifractal techniques should be considered a valuable part of a forest ecologist's toolkit which enable the characterization or differentiation of forest spatial patterns. However, these properties (e.g.,  $f(\alpha)$  spectra) are not calculated because dimensions are intrinsically interesting, but because they represent a potential window to the pattern generating mechanism (Mandelbrot, 1988) such as those resulting from environmental (e.g., distribution of soil moisture or nutrients) factors, exogenous (e.g., natural or anthropogenic disturbance) or endogenous (e.g., successional) processes. Along these lines, Lorimer et al. (1994) discussed the importance of abiotic heterogeneity in producing different fractal distributions of trees, and Solé and Manrubia (1995) showed via a cellular automata gap model how changes in biotic processes (i.e., mortality probability) may result in different overall multifractal patterns of forested landscapes. Hence, in order to determine the inherent causes of naturally occurring multifractal patterns in forested systems, models that couple a template of underlying multifractal generating abiotic conditions

with multifractal generating biotic factors need to be developed.

## Acknowledgements

We wish to thank David Harding and the Laser Altimeter Processing Facility at NASA Goddard Space Flight Center for providing the SLICER data, the DWP for GIS layers and permission to use their preserve, and Jason Godin, George Husk, and Jon Sloan for field assistance. Support that enabled this study was provided by the NASA Earth Science Enterprise New Investigator Program (NAG-W5202).

## References

- Blair, J.B., Harding, D.J., 1998. SLICER — Scanning Lidar Imager of Canopies by Echo Recovery. Available at: <http://ftpwww.gsfc.nasa.gov/eib/slicer.html>.
- Brockway, D.G., Outcalt, K.W., 1998. Gap-phase regeneration in longleaf pine wiregrass ecosystems. *For. Ecol. Manage.* 106, 125–139.
- Falconer, K.J., 1990. *Fractal Geometry: Mathematical Foundations and Applications*. Wiley, New York, p. 288.
- Keitt, T.H., 1996. Spectral representation of neutral landscapes. Available at: <http://www.santafe.edu/sfi/publications/96wplist.html>.
- Lefsky, M.A., 1997. Application of lidar remote sensing to the estimation of forest canopy and stand structure. Ph.D. dissertation, University of Virginia, Charlottesville, Virginia.
- Lorimer, N.D., Haight, R.G., Leary, R.A., 1994. *The Fractal Forest: Fractal Geometry and Applications in Forest Science*. NC-170, US Department of Agriculture, Forest Service, St. Paul, Minnesota.
- Mach, J., Mas, F., 1997. MFRAC v2.0 Software for fractal and multifractal indices calculation. Available at: <http://www.qf.ub.es/area5/jordi/mfrac.html>.
- Mandelbrot, B.B., 1988. An introduction to multifractal distribution functions. In: Stanley, H.E., Ostrowsky, N. (Eds.), *Random Fluctuations and Pattern Growth: Experiments and Models*. Kluwer Academic Publishers, Dordrecht, Netherlands, pp. 279–291.
- Milne, B.T., 1991. Lessons from applying fractal models to landscape patterns. In: Turner, M.G., Gardner, R.H. (Eds.), *Quantitative Methods in Landscape Ecology*. Springer, New York, pp. 199–235.
- Nelson, R., Krabill, W., Maclean, G., 1988. Using airborne lasers to estimate forest canopy and stand characteristics. *J. For.* 86, 31–38.
- Pachepsky, Y.A., Ritchie, J.C., Gimenez, D., 1997. Fractal modeling of airborne laser altimetry data. *Remote Sens. Environ.* 61, 150–161.
- Pecknold, S., Lovejoy, S., Schertzer, D., Hooge, C., 1997. Multifractals and resolution dependence of remotely sensed data: GSI to GIS. In: Quattrochi, D.A., Goodchild, M.F. (Eds.), *Scale in Remote Sensing and GIS*. CRC Press, Boca Raton, FL, pp. 361–394.
- Platt, W.J., Evans, G.W., Rathbun, S.L., 1988. The population dynamics of a long-lived conifer (*Pinus palustris*). *The Am. Naturalist* 131, 491–525.
- Solé, R.V., Manrubia, S.C., 1995. Are rainforests self-organized in a critical state? *J. Theor. Biol.* 173, 31–40.
- Tilman, D., Kareiva, P., 1997. *Spatial Ecology: The Role of Space in Population Dynamics and Interspecific Interactions*. Princeton University Press, Princeton, p. 368.
- Vedyushkin, M.A., 1994. Fractal properties of forest spatial structure. *Vegetatio* 113, 65–70.
- Weishampel, J.F., Harding, D.J., Boutet, J.C., Drake, J.B., 1997. Analysis of laser altimeter waveforms for forested ecosystems of Central Florida. In: Narayanan, R.M., Kalshoven Jr., J.E. (Eds.), *Advances in Laser Remote Sensing for Terrestrial and Oceanographic Applications*. Proceedings of SPIE, vol. 3059, pp. 184–189.
- Zeide, B., 1991. Fractal geometry in forestry applications. *For. Ecol. Manage.* 46, 179–188.